Turkish Journal of Science & Technology
Volume 12(2), 1-21, 2017

Fractal Analysis of Shear-thinning Fluid Flow through Porous Media

Fethi KAMIŞLI
Department of Chemical Engineering, Fırat University, Elazığ, Turkey.
fkamisli@firat.edu.tr

(**Received: 17. 01. 2017; Accepted: 10. 05. 2017**)

Abstract

Keywords: Shear-thinning fluid, Porous media, Packed bed, Permeability, Fractal modeling,

Gözenekli Ortamda Kayma İnceltmeli Akışkan Akışının Fraktal Analizi

Özet

Newtonian, üs kanunu, Ellis ve Bingham akışkanlarının dolgulu yataklarda hacimsel debilerinin ve geçirgenliklerinin hesaplanması için fraktal modeller, kıvrımlı kanalların fraktal doğası göz önünde bulundurularak geliştirilmiştir. Newtonian ve Newtonian olmayan akışkanlar için fraktal geçirgenlik modeller, kıvrımlılığın fraktal boyutuna, gözenek alanının fraktal boyutuna, taneciklerin ve kümelerin büyüklüğüne, etkin gözeneklilige ve Newtonian olmayan akış davranışına bağlı olduğu bulunmuştur. Basıncın fonksiyonu olarak herbir akışkanın hacimsel debisi hem yakınsaklık-ıraksaklık yaklaşımından hem de modellerin birbiriyle kıyaslanması için geliştirilen ifadeden hesaplanmıştır. Dahası, hidrolik temaslılık fraktal ölçeklendirme parametresi cinsinden ayrıca elde edilmiştir. Üs kanunu ve Ellis akışkanlarını da içine alan kayma inceltmeli akışkanların hacimsel debileri kıvrımlık fraktal boyutunun artmasıyla azalmaktadır. Newtonian ve Ellis akışkanları için fraktal kılcal model, incelenen kıvrımlılık fraktal boyut değerleri için, yakınsaklık-ıraksaklık kanal yaklaşımı ile uyumlu olduğu bulunmuştur.

Anahtar kelimeler: Kayma inceltmeli akışkan, Gözenekli ortamlar, Dolgulu yatak, Geçirgenlik, Fraktal modelleme.

1. Introduction

The flow of fluids through porous media is of great practical importance in many diverse applications, including the production of oil and gas from geological structures, the gasification of coal, the retorting of shale oil, filtration, ground water movement, regenerative heat exchange, surface catalysis of chemical reactions, adsorption, coalescence, dying ion exchange, and chromatography. Some applications mentioned above involve two or even three fluids, and multidimensional and unsteady flows. Attention here will be confined to steady one-dimensional flow of a single fluid relative to a fixed solid phase. In some applications, the details of volumetric flow rate and thus velocity field are of concern.

In recent years there has been considerable interest shown in the flow of a non-Newtonian fluid in porous media. A lot of liquids encountered in daily life such as most of polymeric liquids, milk, blood and some oil products and their derivative are non-Newtonian. Therefore, the flows of non-Newtonian fluids in porous media are important and have several applications including oil recovery, composite material processing and polymer processing. The creeping flows of Newtonian fluids in porous media such as granular media or packed bed have been studied for several years and have good constitutive equations namely Darcy's law, the Ergun equation and Blake-Kozeny equation. However, the mentioned constitutive equations are not applicable for non-Newtonian fluids or do not give as good results for non-Newtonian fluid as Newtonian ones.

Darcy's law was modified by Bird et al. [1] and Sabiri and Comiti [2] to obtain an equation valid for non-Newtonian fluid flows in porous

media. The majority of these models have been derived using the bundle-of-tube approximation employed in the Blake-Kozeny model.

The Saffman-Taylor instability of air invasion into a non-Newtonian fluid in a rectangular Hele-Show cell was experimentally studied by Eslami and Taghavi [3]. The non-Newtonian fluid used in the experiments exhibited yield stress, shear-thinning as well as elastic behaviors. They observed that the Bingham number (Ba), the capillary number (Ca), the Weber number (We), the Weissenberg number (Wi), the power-law index and channel aspect ratio ($\delta >>1$) are important parameters on viscous flow regimes.

Rheological characterization of biologically immobilized aggregates under non-Newtonian flow was studied by Tijani et al. [4]. They concluded that the scaling relationships based on fractal geometry are vital for quantifying the effects of different laminar conditions on the aggregates' morphology and characteristics such as density, porosity and projected surface area.

The viscous fingering instability of miscible displacement involving a viscoelastic fluid was investigated by Shokri et al. [5] using both linear stability analysis and computational fluid dynamics. They observed that the elasticity has a significant effect on the fingering instability and the flow was more stabilized when elasticity (Weissenberg number) of the displaced or displacing viscoelastic fluid was increased.

As stated previously, flows of non-Newtonian fluids in porous media have been studied for several years. Balhoff and Thompson [6] developed a macroscopic model for the flow of power-law and Ellis fluids in packed beds using results from the network model based on the functionality of flow in capillary tubes. The model is in general similar to those developed using the bundle-of-tubes approach. They claimed that a developed bundle-of-tubes model cannot be properly used for a wide variety of shear-thinning fluids.

Chhabra et al. [7] published a review paper on the flow of rheologically complex fluids through unconsolidated fixed beds and fluidized beds. They critically evaluated the prediction of macro-scale phenomena of flow regimes, pressure drop in fixed and fluidized beds, minimum fluidization velocity, dispersion and liquid-solid mass transfer.

On the other hand, Yu and Liu [8] developed the fractal-phase permeability and the relative permeability based on the fractal nature of pores in the media. Both the fractal-phase permeability and the relative permeability were found to be a function of the tortuosity fractal dimension, the pore-area fractal dimension, the phase fractal dimension and microstructural parameters. In another study a fractal permeability model based on the fractal characteristics of pores was developed for bi-dispersed porous media by Yu and Cheng [9].

The flowrate of non-Newtonian fluids depends on the pressure drop, rheological properties of the fluid, and geometry of the duct. It may be possible to develop complicated empirical correlations using these variables and data obtained from CFD modeling. Shear-thinning behavior, viscoelasticity, yield stress, time-dependency etc. are features for the most of non-Newtonian materials. However, some of these features such as time-dependent viscosity, yields stress etc. are seldom measured. The development of simple and reliable methods for predicting flowrates of power-law, Ellis and Bingham fluids flowing through packed beds has been subject for many researchers.

As expressed earlier, Balhoff and Thompson [6] developed approximate equations specific to the flow of shear-thinning fluids in ducts that are representative of throats in the network. They also indicated that some drawbacks exist in the approach of the capillary networks. In theory each throat could be transformed into a unique capillary tube and the resulting capillary network could be used to properly model flow for that specific power-law fluid although this may seem like a reasonable approach, several problems exist with method proposed by Balhoff and Thompson [6].

There is no guarantee that the same capillary network could be used for another power-law fluid with different rheological properties.

An entirely new capillary network would have to be developed to model the flow of other non-Newtonian fluids since the capillary network could not be used for non-Newtonian fluid models

such as Bingham and Herschel-Bulkly models and others.

In many situations, it is highly desirable to obtain closed-form equations analogous to Darcy's law to predict the volumetric flow rate of non-Newtonian fluids in porous media.

Therefore, the goal in this study is to develop closed-form equations analogous to Darcy's law to predict the flow rates and permeabilities for non-Newtonian fluids in porous media. The fractal capillary expressions are developed based on the fractal nature of tortuous capillaries for the volumetric flow rates and permeabilities for Newtonian, power-law and Ellis fluids. The computed flow rates from the present model for the considered fluids are compared to theoretical work and data available in the literature and a good agreement for some fluid models is found.

2. Theoretical

Many polymers and suspensions are non-Newtonian, exhibiting shear-dependent viscosity. Therefore, in this subsection it will be given some information regarding models of non-Newtonian fluids that are commonly used in the porous media or any other engineering field. The most successful attempts at describing the steady stress-shear rate behavior of non-Newtonian fluids have been largely empirical. It would be much more satisfying if one could derive these functions from theories based on molecular structure, but most of the materials of greatest interest are extremely complex and generally inadequate for describing real behavior. Hence, at present observations represent the most reliable source of rheological information. The following represents some of the more common empirical models which have been utilized to represent the various classes of observed non-Newtonian behavior.

Power-law model

The relationship between shear stress-shear rate for a power-law fluid is given by

$$\tau = -m\left|\dot{\gamma}\right|^{n-1}\dot{\gamma} \quad \text{and} \quad \eta = m\left|\dot{\gamma}\right|^{n-1}$$

where n is power-law index, m consistency index and η shear dependent viscosity of power-law fluid. The power-law model is the most widely used of any model, since it is relatively easy to incorporate into analytical solutions to flow problems, and it can be made to fit almost any data over a limited range of shear rate. In the model the viscosity is also given above. The model predicts that τ vs $\dot{\gamma}$ is straight line on the double logarithmic plot. If the shear rate does not vary widely over a particular flow field, the power-law may provide an adequate description of shear behavior. However, it has two serious drawbacks. For constant values of n and m, it predicts unlimited increasing or decreasing apparent viscosity with shear rate; and it predicts either zero or infinite values in the limit of vanishing shear rate for n greater or less than 1, respectively. This, of course, is not observed in real fluids.

The volumetric flow rate for the power-law fluid can be obtained by integrating the velocity expression the z-direction with respect to r on the cross-sectional area of the capillary as follows:

$$q = \left[\frac{(n\pi)^n R^{3n+1}}{(3n+1)^n\, 2m}\left(-\frac{dp}{dz}\right)\right]^{1/n} \tag{1}$$

The volumetric flow rate equation for the flow of a power-law fluid through a tortuous capillary tube can be written in the form of Eq. (1). As can be seen from the above equation the flow rate of a power-law fluid must be proportional to the pressure gradient to the power of $1/n$ ($q \propto (dp/dz)^{1/n}$) for a capillary tube. Eq. (1) has to be valid for any capillary tube with slowly-varying radius along the axial direction. In this connection Pearson and Tardy [10] stated that for any geometry the flow rate of power-law fluid must be proportional with the pressure drop to the power of $1/n$ ($q \propto \Delta p^{1/n}$). Therefore, it can be said that a capillary tube must exist that produces some flow rate versus pressure drop as in the original porous medium for a fluid with rheological properties n and m.

Ellis model

The Ellis model uses three parameters. At low shear rates this model approaches Newtonian

behavior with a zero shear viscosity, η_0. At high shear rates power-law behavior is approached with *n* corresponding to the flow index. In comparison to the power-law the Ellis model is slightly more complicated algebraically, and requires the measurement of an additional parameter. It fits data over a wider range of shear rate than the power-law does, and does not suffer from the *zero shear failure*, the prediction of infinite viscosity at zero shear rates. The Ellis model has been widely used in attempts to describe complex flow of shear-thinning fluids. The shear thinning fluid is defined as of the viscosity decreases with increasing shear rate.

The volumetric flow rate for a non-Newtonian fluid described by Ellis model can be obtained by integrating the velocity expression in the z-direction on the cross-sectional area of a capillary tube as follows:

$$q=\frac{\pi R^4}{8\eta_0}\left(-\frac{dp}{dz}\right)\left[1+\frac{4}{(\alpha+3)}\left(-\frac{R}{2\tau_{1/2}}\frac{dp}{dz}\right)^{\alpha-1}\right] \quad (2)$$

where η_0 is the low shear viscosity, α flow (power) index in the Ellis model and $\tau_{1/2}$ rheological parameter in the model, respectively. Eq. (2) gives the volumetric flow rate of the Ellis fluid as a function of the pressure drop, flow index, viscosity of fluid and radius of the capillary tube. As can be seen from Eq. (2) an increase in the pressure gradient in the sufficient level which is equivalent to the sufficiently high shear rate will make the second term in the parenthesis much lower as comparing to the first term, unity. Therefore, the first term in the parenthesis can be neglected and thus the equation becomes equal to the volumetric flow rate of power-law fluid. On the other hand, the low pressure gradient which is equivalent to the low shear rate will make the second term in the parenthesis much lower as comparing to the first term, unity. Hence the second term in the parenthesis can be dropped and thus the equation reduces to the volumetric flow rate of a Newtonian fluid in a capillary tube.

Bingham plastic model

One class fluids, including toothpastes, oil-well drilling mud, sewage sludge, oil paints, margarines, plastic melts, aqueous suspensions of clay, grain and paper pulps, chocolate syrups, aqueous slurries of coal, peat, sand and cement require a finite shear stress to produce any motion. Such fluids are known as Bingham plastics.

The constitutive equation for Bingham plastic model is given by

$$\tau_{rz}=\pm\tau_0-\mu\frac{dv_z}{dr} \qquad |\tau_{rz}|>\tau_0 \quad (3)$$

$$\frac{dv_z}{dr}=0 \text{ for } \quad 0\le|\tau_{rz}|\le\tau_0$$

Where τ_0 is yield stress and μ is effective viscosity for absolute values of the shear stress in excess of the yield stress. The arbitrary sign preceding τ_0 in Eq. (3) is chosen to be the same as the actual sign of τ_{rz}. Thus if $\tau_{rz}>0$, the plus sign is chosen, and vice versa. A Bingham plastic does not flow below a certain yield stress τ_0. When this stress is exceeded, the structure disintegrates and the material behaves like a Newtonian fluid.

The volumetric flow rate for Bingham fluid in a capillary tube consists of the volumetric flow rate obtained by integrating the r-dependent velocity expression with respect to *r* over the cross-sectional area between r_0 and *R* plus the flow rate obtained by use of the constant velocity multiplied with the corresponding cross-sectional area. Therefore, the volumetric flow rate for a non-Newtonian fluid described by Bingham plastic model is obtained as follows:

$$q=\frac{\pi}{8\mu}\left(-\frac{dp}{dz}\right)R^4\left[1-\frac{8}{3R}\frac{\tau_0}{(-dp/dz)}+\frac{1}{3}\left(\frac{2\tau_0}{R(-dp/dz)}\right)^4\right] \quad (4)$$

The obtained volumetric flow rate equations for Newtonian and non-Newtonian fluid flows through a straight capillary tube can be expressed in terms of the fractal scaling parameters. In order to express volumetric flow rate equations in terms of the fractal scaling parameters, the brief

information regarding to the fractal scaling law is necessary to be given here. Hence the fractal scaling law is briefly explained in the following section.

3. Fractal Theory for Porous Media

A porous medium having various pore sizes can be considered as a bundle of tortuous capillary tubes with variable cross-sectional areas. Let the diameter of a capillary in the medium be λ and its tortuous length along flow direction be $L(\lambda)$. The tortuous nature of capillary requires that $L(\lambda) > L_0$, with L_0 being straight length. For a straight capillary, $L(\lambda) = L_0$. The relationship between the diameter and length of capillaries is given by [9]

$$L = L_0^{D_T} \lambda^{1-D_T} \tag{5}$$

where D_T is the tortuosity fractal dimension, with $1 < D_T < 2$, representing the extent of convolutedness of capillary pathways for fluid flow through a medium. The limiting case of $D_T = 2$, corresponds to a highly tortuous line that fills a plane and Eq. (5) diverges as $\lambda \to 0$, which is one of the properties of fractal line [8,9].

Since the pores in porous media are analogous to the islands or lakes on earth or spots on engineering surfaces, the cumulative size-distribution of pores or islands should also follow the same fractal scaling law. Therefore, a number of islands or pores whose size is larger than λ is given [6 and references therein] by

$$N(L > \lambda) = \left(\frac{\lambda_{\max}}{\lambda} \right)^{D_f} \tag{6}$$

and derivative of Eq. (6) is

$$-dN = D_f \lambda_{\max}^{D_f} \lambda^{-(D_f+1)} d\lambda \tag{7}$$

where D_f is the pore-area fractal dimension having values between 1 and 2 in two dimensional space. The negative sign in Eq. (7) implies that the island or pore population decreases with the increase of island or pore size and $-dN > 0$. The number of pores from Eq. (6) becomes infinity as $\lambda \to 0$, which is one of the properties of fractal objects. The total number of pores, islands or spots, from the smallest diameter $\lambda_{\min}$ to the largest diameter $\lambda_{\max}$, can be obtained from Eq. (6) as

$$N_t(L > \lambda) = \left(\frac{\lambda_{\max}}{\lambda_{\min}} \right)^{D_f} \tag{8}$$

Dividing Eq.(7) by (8) yields

$$-\frac{dN}{N_t} = D_f \lambda_{\min}^{D_f} \lambda^{-(D_f+1)} d\lambda = f(\lambda) d\lambda \tag{9}$$

where $f(\lambda) = D_f \lambda_{\min}^{D_f} \lambda^{-(D_f+1)}$ is the probability density function which satisfies following condition

$$f(\lambda) \geq 0 \tag{10}$$

As in the probability theory, the probability density function $f(\lambda)$, should also satisfies the following relationship.

$$\int_{-\infty}^{\infty} f(\lambda) d\lambda = \int_{\lambda_{min}}^{\lambda_{max}} f(\lambda) d\lambda = 1 \tag{11}$$

However, substituting the probability density function into Eq. (11) and performing integration yields

$$\int_{\lambda_{\min}}^{\lambda_{\max}} D_f \lambda_{\min}^{D_f} \lambda^{-(D_f+1)} d\lambda = 1 - \left(\frac{\lambda_{\min}}{\lambda_{\max}} \right)^{D_f} \tag{12}$$

Therefore, Eq. (11) satisfies if and only if

$$\left(\frac{\lambda_{\min}}{\lambda_{\max}} \right)^{D_f} \cong 0 \tag{13}$$

Eq. (13) implies that $\lambda_{\min} << \lambda_{\max}$ must be satisfied for fractal analysis of a porous medium;

otherwise the porous medium is a non-fractal medium. Thus, Eq. (13) can be considered as a criterion whether a porous medium can be characterized by fractal theory and technique. In general $\lambda_{\min}/\lambda_{\max} < 10^{-2}$ in porous media and Eq. (13) holds approximately. Therefore, the fractal theory and technique can be used to analyze properties of porous media in which the condition of $\lambda_{\min}/\lambda_{\max} < 10^{-2}$ is satisfied.

4. Fractal Permeability for non-Newtonian Fluid Flowing in Capillary Tube

Consider a unit cell consisting of a bundle of tortuous capillary tubes with variable cross-sectional areas. The volumetric flow rate, Q, through the unit cell is a sum of the flow rates through all the individual capillaries. The volumetric flow rate of a power-law fluid flowing through a single capillary tube is given by Eq. (1) that can be modified by taking $-dp = \Delta p$, $dz = L(\lambda)$ and $2R = \lambda$ for a single tortuous capillary tube as follows:

$$q(\lambda) = \left[\left(\frac{n\pi}{3n+1}\right)^n \frac{\lambda^{3n+1}}{2^{3n+2} m} \frac{\Delta P}{L(\lambda)}\right]^{1/n} \tag{14}$$

where λ is the hydraulic diameter of a single capillary tube, m is consistency index in power-law model, ΔP is the pressure drop and $L(\lambda)$ is the length of the tortuous capillary tube.
The volumetric flow rate of a Newtonian fluid flowing through a single tortuous capillary tube is recovered from Eq. (14) by taking $n = 1$ and $m = \mu$ as follows:

$$q(\lambda) = \frac{\pi \Delta P}{128 \mu} \frac{\lambda^4}{L(\lambda)} \tag{15}$$

The total volumetric flow rate, Q, for either a non-Newtonian fluid or a Newtonian fluid can be obtained by integrating the individual volumetric flow rate, $q(\lambda)$, over the entire range of pore sizes from the minimum pore $\lambda_{\min}$ to the maximum pore $\lambda_{\max}$ in a unit cell. The total volumetric flow rate equation for a power-law fluid in a unit cell can be obtained from Eqs. (5), (7) and (14) as follows:

$$Q = \int_{\lambda_{\min}}^{\lambda_{\max}} q(\lambda)\left(-dN(\lambda)\right) = \left[\left(\frac{n\pi}{3n+1}\right)^n \frac{\Delta P}{2^{3n+2} m L_0^{D_T}}\right]^{1/n} D_f \lambda_{\max}^{D_f} \int_{\lambda_{\min}}^{\lambda_{\max}} \lambda^{2+D_T/n-D_f} d\lambda \tag{16}$$

Integrating Eq.(16) yields the total volumetric flow rate of a power-law fluid in a unit cell as follows:

$$Q = \left[\left(\frac{n\pi}{3n+1}\right)^n \frac{\Delta P}{2^{3n+2} m L_0^{D_T}}\right]^{1/n} \frac{D_f}{3 + D_T/n - D_f} \lambda_{\max}^{3+D_T/n} \left[1 - \left(\frac{\lambda_{\min}}{\lambda_{\max}}\right)^{3+D_T/n-D_f}\right] \tag{17}$$

Since $1 < D_T < 2$, $1 < D_f < 2$ and $0 < n < 1$, in any case exponent $3 + D_T/n - D_f > 0$ and $\lambda_{\min}/\lambda_{\max} \approx 10^{-2}$ is criterion for typical fractal geometry. Therefore, the inside of the second bracket is approximately equal to 1. Consequently, the total volumetric flow rate of a power-law fluid become

$$Q=\left[\left(\frac{n\pi}{3n+1}\right)^{n}\frac{\Delta P}{2^{3n+2}mL_0^{D_T}}\right]^{1/n}\frac{D_f}{3+D_T/n-D_f}\lambda_{\max}^{3+D_T/n} \tag{18}$$

Note that the total volumetric flow rate of a Newtonian fluid is recovered from Eq. (18) by taking $n=1$ and $m=\lambda$ as follows:

$$Q=\frac{\pi\Delta P}{128\mu L_0^{D_T}}\frac{D_f}{3+D_T-D_f}\lambda_{\max}^{3+D_T} \tag{19}$$

The permeability expressions for a power-law fluid and a Newtonian in the porous medium are obtained using Darcy's law as follows:

$$K_M=\frac{Q}{\left(\Delta P\,A/\left(L_0 m\right)\right)^{1/n}}=\left[\left(\frac{n\pi}{3n+1}\right)^{n}\frac{1}{2^{3n+2}L_0^{D_T-1}A}\right]^{1/n}\frac{D_f}{3+D_T/n-D_f}\lambda_{\max}^{3+D_T/n} \tag{20}$$

In this equation K_M is the permeability for a power-law fluid that is a function of the pore-area fractal dimension, D_f, the tortuosity fractal dimension, D_T, the power-law index, n, and the structural parameters, A, L_0 and $\lambda_{\max}$. The permeability expression for a Newtonian fluid flowing through porous medium is again recovered from Eq. (20) by taking $n=1$ and $m=\lambda$ as follows:

$$K=\frac{Q}{\left(\Delta P\,A/\left(L_0 m\right)\right)}=\frac{\pi}{128AL_0^{D_T-1}}\frac{D_f}{3+D_T-D_f}\lambda_{\max}^{3+D_T} \tag{21}$$

Eq. (21) had been derived by Yu and Cheng [8, 9] for a Newtonian in a porous unit cell. Eq. (21) points out that the permeability for a Newtonian fluid is a function of the pore-area fractal dimension, D_f, the tortuosity fractal dimension, D_T and the structural parameters, A, L_0 and $\lambda_{\max}$.If the tortuous capillary tube is considered to be a straight capillary tube (D_T =1), the Eqs. (18) and (20) reduce to the following equations, respectively.

$$Q=\left[\left(\frac{n\pi}{3n+1}\right)^{n}\frac{\Delta P}{2^{3n+2}mL_0}\right]^{1/n}\frac{D_f}{3+1/n-D_f}\lambda_{\max}^{3+1/n} \tag{22}$$

$$K_M=\left[\left(\frac{n\pi}{3n+1}\right)^{n}\frac{1}{2^{3n+2}A}\right]^{1/n}\frac{D_f}{3+1/n-D_f}\lambda_{\max}^{3+1/n} \tag{23}$$

The above equations for the Newtonian case become

$$Q=\frac{\pi\Delta P}{128\mu L_0}\frac{D_f}{4-D_f}\lambda_{\max}^{4} \tag{24}$$

$$K=\frac{\pi}{128A}\frac{D_f}{4-D_f}\lambda_{\max}^{4} \tag{25}$$

Eqs.(18)-(25) indicate that the volumetric flow rate and permeability for power-law fluids and Newtonian fluids are very sensitive to the maximum pore size $\lambda_{\max}$. Eqs. (22) and (23) point out that the effects of process variables on the volumetric flow rate and permeability for a power-law fluid. The larger pore diameter and pore-area fractal dimension D_f, the larger volumetric flow rate and permeability value. If it

is assumed that the consistency index, m, is constant while the power-law index changes, the larger power-law index having value between 0 and 1, the larger volumetric flow rate and permeability value. From Eqs. (22)–(25) it can be seen that the volumetric flow rate and permeability for power-law and Newtonian fluids will reach possible maximum values as the pore-area fractal dimension approaches its possible maximum value of 2 since those quantities, as stated earlier, increase with increasing pore diameter. The pore-area fractal dimension $D_f = 2$ corresponds to a smooth surface or plane or compact cluster [9]. This means that if it is considered a smooth surface or compact cluster or a circle or a square to be the cross-sectional area of a pore, the pore-area fractal dimension of the cross-section is 2 and the pore volume fraction of the cross-section is 1. Under such a condition the volumetric flow rate and permeability for both fluid cases take their maximum values. Hence, the maximum volumetric flow rate and permeability for a power-law fluid flowing through the unit cell with a single capillary tube or pore are obtained from Eqs. (22) and (23) as the pore-area fractal dimension, D_f, takes its maximum value of 2.

$$Q = \left[\left(\frac{n\pi}{3n+1}\right)^n \frac{\Delta P}{2^{3n+2} m L_0}\right]^{1/n} \frac{2}{3+1/n-2} \lambda_{\max}^{3+1/n} = \left[\left(\frac{n\pi}{3n+1}\right)^n \frac{\Delta P}{2^{3n+2} m L_0}\right]^{1/n} \frac{2}{3+1/n-2} De^{3+1/n} \tag{26}$$

$$K_M = \left[\left(\frac{n\pi}{3n+1}\right)^n \frac{1}{2^{3n+2} A}\right]^{1/n} \frac{2}{3+1/n-2} \lambda_{\max}^{3+1/n} = \left[\left(\frac{n\pi}{3n+1}\right)^n \frac{1}{2^{3n} \pi}\right]^{1/n} \frac{2}{3+1/n-2} De^{(3n-1)/n} \tag{27}$$

For the case of Newtonian fluids, the above equations reduce to the following equations.

$$Q = \frac{\pi \Delta P}{128 \mu L_0} De^4 = \frac{A \Delta P}{32 \mu L_0} De^2 \tag{28}$$

where De can be called equivalent diameter of a unit cell and is taken to be equal to $\lambda_{\max}$.

$$K = \frac{\pi}{128 A} \lambda_{\max}^4 = \frac{De^2}{32} \tag{29}$$

Eq. (28) indicates that the present model for power-law and Newtonian fluids is consistent with the physical situation since it is exactly the Hangen-Poiseuille equation for a Newtonian fluid flow through a tube. Therefore, besides Eqs. (28)-(29), Eq. (15) with $D_T = 1$ (and thus $L = L_0$) can be used for obtaining the volumetric flow rate and permeability for a Newtonian fluid flow through the unit cell with a straight capillary tube. However, the volumetric flow rate equation (Eq. 14) developed for a power-law fluid flow through a tube can't be used for obtaining volumetric flow rate of that fluid flow through the unit cell with a straight capillary tube since Eq. (14) with $D_T = 1$ (and thus $L = L_0$) isn't entirely equal to Eq. (26). The volumetric flow rate, Q, through the unit cell is a sum of the flow rates through all the individual capillaries. The volumetric flow rate of an Ellis fluid flowing through a single capillary tube is given by Eq. (2) that can be modified by taking $-dp = \Delta p$, $dz = L(\lambda)$ and $2R = \lambda$ for a single tortuous capillary tube as follows:

$$q(\lambda) = \frac{\pi \lambda^4}{128 \eta_0} \frac{\Delta P}{L(\lambda)} \left[1 + \frac{4}{(\alpha+3)} \left(\frac{\lambda}{4\tau_{1/2}} \frac{\Delta P}{L(\lambda)}\right)^{\alpha-1}\right] \tag{30}$$

where λ is the hydraulic diameter of a single capillary tube, η_0 is the low shear viscosity of Ellis Fluid, $\tau_{1/2}$ is the rheological parameter, ΔP is the pressure drop and $L(\lambda)$ is the length of the tortuous capillary tube.

The total volumetric flow rate, Q, for either a non-Newtonian fluid or a Newtonian fluid can

be obtained by integrating the individual volumetric flow rate, $q(\lambda)$, over the entire range of pore sizes from the minimum pore $\lambda_{\min}$ to the maximum pore $\lambda_{\max}$ in a unit cell. The total volumetric flow rate equation for an Ellis fluid in a unit cell can be obtained from Eqs. (5), (7) and (30) as follows:

$$Q=\int_{\lambda_{\min}}^{\lambda_{\max}} q(\lambda)\left(-dN(\lambda)\right)=\frac{\pi\,\Delta P}{128\eta_0\,L_0^{D_T}}D_f\,\lambda_{\max}^{D_f}\int_{\lambda_{\min}}^{\lambda_{\max}}\left[\lambda^{2+D_T-D_f}+4\left(\frac{\Delta P}{4\tau_{1/2}\,L_0^{D_T}}\right)^{\alpha-1}\frac{\lambda^{2+\alpha D_T-D_f}}{\alpha+3}\right]d\lambda \tag{31}$$

Integrating Eq.(31) yields the total volumetric flow rate of an Ellis fluid in a unit cell as follows:

$$Q=\frac{\pi\,\Delta P}{128\eta_0\,L_0^{D_T}}D_f\,\lambda_{\max}^{D_f}\left[\frac{\lambda_{\max}^{3+D_T}}{3+D_T-D_f}\left(1-\left(\frac{\lambda_{\min}}{\lambda_{\max}}\right)^{3+D_T-D_f}\right)+\frac{4\,\lambda_{\max}^{3+\alpha D_T}}{(\alpha+3)(3+\alpha D_T-D_f)}\left(\frac{\Delta P}{4\tau_{1/2}\,L_0^{D_T}}\right)^{\alpha-1}\left(1-\left(\frac{\lambda_{\min}}{\lambda_{\max}}\right)^{3+\alpha D_T-D_f}\right)\right] \tag{32}$$

Since $1<D_T<2$ and $1<D_f<2$, in any case exponent $3+D_T-D_f>0$ and $3+\alpha D_T-D_f>0$ and $\lambda_{\min}/\lambda_{\max}\approx 10^{-2}$ is criterion for typical fractal geometry. Therefore, the ratio of $\lambda_{\min}/\lambda_{\max}$ is negligible in the above equation. In other words, the insides of the parentheses are approximately equal to 1. Consequently, the total volumetric flow rate of an Ellis fluid becomes

$$Q=\frac{\pi\,\Delta P\,\lambda_{\max}^{3+D_T}}{128\eta_0\,L_0^{D_T}}\frac{D_f}{3+D_T-D_f}\left[1+\frac{4\left(3+D_T-D_f\right)}{(\alpha+3)(3+\alpha D_T-D_f)}\left(\frac{\lambda_{\max}^{D_T}\,\Delta P}{4\tau_{1/2}\,L_0^{D_T}}\right)^{\alpha-1}\right] \tag{33}$$

The permeability expressions for an Ellis fluid in the porous medium are obtained using Darcy's law as follows:

$$K=\frac{Q}{\left(\Delta PA/\left(L_0\eta_0\right)\right)}=\frac{\pi\;\lambda_{\max}^{3+D_T}}{128A\;L_0^{D_T-1}}\frac{D_f}{3+D_T-D_f}\left[1+\frac{4\left(3+D_T-D_f\right)}{(\alpha+3)(3+\alpha D_T-D_f)}\left(\frac{\lambda_{\max}^{D_T}\,\Delta P}{4\tau_{1/2}\,L_0^{D_T}}\right)^{\alpha-1}\right] \tag{34}$$

K is the permeability for an Ellis fluid that is a function of the pore-area fractal dimension, D_f, the tortuosity fractal dimension, D_T, the flow index, α, rheological parameter, $\tau_{1/2}$, and the structural parameters, A, L_0 and $\lambda_{\max}$. If the tortuous capillary tube is considered to be a straight capillary tube (D_T =1), the Eqs. (33) and (34) reduce to the following equations, respectively.

$$Q = \frac{\pi \Delta P \lambda_{\max}^4}{128 \eta_0 L_0} \frac{D_f}{4 - D_f} \left[1 + \frac{4\left(4 - D_f\right)}{\left(\alpha + 3\right)\left(3 + \alpha - D_f\right)} \left(\frac{\lambda_{\max} \Delta P}{4 \tau_{1/2} L_0} \right)^{\alpha - 1} \right] \tag{35}$$

$$K = \frac{\pi \lambda_{\max}^4}{128 A} \frac{D_f}{4 - D_f} \left[1 + \frac{4\left(4 - D_f\right)}{\left(\alpha + 3\right)\left(3 + \alpha - D_f\right)} \left(\frac{\lambda_{\max} \Delta P}{4 \tau_{1/2} L_0} \right)^{\alpha - 1} \right] \tag{36}$$

Eqs.(33)-(36) indicate that the volumetric flow rate and permeability for an Ellis fluid are very sensitive to the maximum pore size $\lambda_{\max}$ as in the power-law and Newtonian fluids. Eqs. (35) and (36) show that the effects of process variables on the volumetric flow rate and permeability for an Ellis fluid. The larger pore diameter and pore-area fractal dimension D_f, the larger volumetric flow rate and permeability value. Furthermore, the larger flow index, the larger volumetric flow rate and permeability value. Eqs. (35)–(36) indicate that the volumetric flow rate and permeability for an Ellis fluid will reach possible maximum values as the pore-area fractal dimension approaches its possible maximum value of 2 since those quantities, as stated earlier, increase with increasing pore diameter. The pore-area fractal dimension $D_f = 2$ corresponds to a smooth surface or plane or compact cluster [9]. This means that if it is considered a smooth surface or compact cluster or a circle or a square to be the cross-sectional area of a pore, the pore-area fractal dimension of the cross-section is 2 and the pore volume fraction of the cross-section is 1. Under such a condition the volumetric flow rate and permeability for Ellis model take their maximum values. Hence, the maximum volumetric flow rate and permeability for an Ellis fluid flowing through the unit cell with a single capillary tube or pore are obtained from Eqs. (35) and (36) as the pore-area fractal dimension, D_f, takes its maximum value of 2.

$$Q = \frac{\pi \Delta P \lambda_{\max}^4}{128 \eta_0 L_0} \left[1 + \frac{8}{\left(\alpha + 3\right)\left(1 + \alpha\right)} \left(\frac{\lambda_{\max} \Delta P}{4 \tau_{1/2} L_0} \right)^{\alpha - 1} \right] \tag{37}$$

$$K = \frac{\pi \lambda_{\max}^4}{128 A} \left[1 + \frac{8}{\left(\alpha + 3\right)\left(1 + \alpha\right)} \left(\frac{\lambda_{\max} \Delta P}{4 \tau_{1/2} L_0} \right)^{\alpha - 1} \right] \tag{38}$$

Eq. (37) is exactly the same as Eq. (30) with $D_T = 1$ (and thus L = L0) for the limiting values of α = 0, 1 and 2. Therefore, the present model is consistent with the physical situation. Hence, besides Eqs. (37)-(38), Eq. (30) with $D_T = 1$ (and consequently L = L0) can be used for obtaining the volumetric flow rate and permeability for an Ellis fluid flow through the unit cell with a straight capillary tube as α takes the values of 0, 1 and 2. Eq. (30) can't be used for obtaining volumetric flow rate of an Ellis fluid flow through the unit cell with a straight capillary tube when □ takes a value other than the values of 0, 1 and 2.

As stated previously, the volumetric flow rate, Q, through the unit cell is a sum of the flow rates through all the individual capillaries. The volumetric flow rate of a Bingham fluid flowing through a single capillary tube is given by Eq. (4) that can be modified by taking $-dp = \Delta p$, $dz = L(\lambda)$ and $2R = \lambda$ for a single tortuous capillary tube as follows:

$$q(\lambda) = \frac{\pi \lambda^4}{128 \mu} \frac{\Delta P}{L(\lambda)} \left[1 - \frac{16 \tau_0}{3 \lambda \left(\Delta P / L(\lambda) \right)} + \frac{1}{3} \left(\frac{4 \tau_0}{\lambda \Delta P / L(\lambda)} \right)^4 \right] \tag{39}$$

where λ is the hydraulic diameter of a single capillary tube, μ is the effective viscosity for absolute values of the shear stress in excess of the yield stress, τ_0 is the yield stress, ΔP is the pressure drop and $L(\lambda)$ is the length of the tortuous capillary tube. The total volumetric flow rate, Q, for either a non-Newtonian fluid or a Newtonian fluid can be obtained by integrating the individual volumetric flow rate, $q(\lambda)$, over the entire range of pore sizes from the minimum pore $\lambda_{\min}$ to the maximum pore $\lambda_{\max}$ in a unit cell. The total volumetric flow rate equation for a Bingham fluid in a unit cell can be obtained from Eqs. (5), (7) and (39) as follows:

$$Q = \int_{\lambda_{\min}}^{\lambda_{\max}} q(\lambda)(-dN(\lambda))$$

$$= \frac{\pi \Delta P}{128 \mu L_0^{D_T}} D_f \lambda_{\max}^{D_f} \int_{\lambda_{\min}}^{\lambda_{\max}} \left[\lambda^{2+D_T-D_f} - \frac{16\tau_0 L_0^{D_T}}{3\Delta P} \lambda^{2-D_f} + \frac{1}{3}\left(\frac{4\tau_0 L_0^{D_T}}{\Delta P} \right)^4 \lambda^{2-3D_T-D_f} \right] d\lambda \tag{40}$$

Integrating Eq. (40) gives the total volumetric flow rate of a Bingham fluid versus pressure drop in a unit cell as follows:

$$Q = \frac{\pi \Delta P}{128 \mu L_0^{D_T}} \frac{D_f \lambda_{\max}^{3+D_T}}{3+D_T-D_f} \left[1 - \left(\frac{\lambda_{\min}}{\lambda_{\max}} \right)^{3+D_T-D_f} - \frac{16\tau_0 L_0^{D_T}}{3\Delta P \lambda_{\max}^{D_T}} \frac{3+D_T-D_f}{3-D_f} \left(1 - \left(\frac{\lambda_{\min}}{\lambda_{\max}} \right)^{3-D_f} \right) \right.$$

$$\left. + \frac{1}{3} \frac{3+D_T-D_f}{(3-3D_T-D_f)} \left(\frac{4\tau_0 L_0^{D_T}}{\Delta P \lambda_{\max}^{D_T}} \right)^4 \left(1 - \left(\frac{\lambda_{\min}}{\lambda_{\max}} \right)^{3-3D_T-D_f} \right) \right] \tag{41}$$

Since $1 < D_T < 2$ and $1 < D_f < 2$, in any case exponent $3+D_T-D_f > 0$ and $3-D_f > 0$ and $3-3D_T-D_f < 0$. By considering the criterion, $\lambda_{\min}/\lambda_{\max} \approx 10^{-2}$, for a typical fractal geometry the terms $\lambda_{\min}/\lambda_{\max}$ with the exponents $3+D_T-D_f > 0$ and $3-D_f > 0$ is negligible in the above equation. However, as $\lambda_{\min}/\lambda_{\max}$ is equal to 10-2, the term $\lambda_{\min}/\lambda_{\max}$ with the exponents $3-3D_T-D_f < 0$ goes to an unacceptable large value that can be considered as an unrealistic physical situation. Under the light of above arguments, the total volumetric flow rate of a Bingham fluid becomes

$$Q = \frac{\pi \Delta P}{128 \mu L_0^{D_T}} \frac{D_f \lambda_{\max}^{3+D_T}}{3+D_T-D_f} \left[1 - \frac{16\tau_0 L_0^{D_T}}{3\Delta P \lambda_{\max}^{D_T}} \frac{3+D_T-D_f}{3-D_f} \right.$$

$$\left. + \frac{1}{3} \frac{3+D_T-D_f}{(3-3D_T-D_f)} \left(\frac{4\tau_0 L_0^{D_T}}{\Delta P \lambda_{\max}^{D_T}} \right)^4 \left(1 - \left(\frac{\lambda_{\min}}{\lambda_{\max}} \right)^{3-3D_T-D_f} \right) \right] \tag{42}$$

The permeability expressions for a Bingham fluid in the porous medium are obtained using Darcy's law as follows

$$K=\frac{Q}{\left(\Delta PA/\left(L_0\mu\right)\right)}=\frac{\pi\ \lambda_{\max}^{3+D_T}}{128A\ L_0^{D_T-1}}\frac{D_f}{3+D_T-D_f}\left[1-\frac{16L_0^{D_T}\tau_0\left(3+D_T-D_f\right)}{3\left(3-D_f\right)\lambda_{\max}^{D_T}\Delta P}\right.$$
$$\left.+\frac{1}{3}\frac{\left(3+D_T-D_f\right)}{\left(3-3D_T-D_f\right)}\left(\frac{4\tau_0\ L_0^{D_T}}{\lambda_{\max}^{D_T}\Delta P}\right)^4\left(1-\left(\frac{\lambda_{\min}}{\lambda_{\max}}\right)^{3-3D_T-D_f}\right)\right] \tag{43}$$

K is the permeability for a Bingham that is a function of the pore-area fractal dimension, D_f, the tortousity fractal dimension, D_T, the yield stress, τ_0, and the structural parameters, A, L_0, $\lambda_{\min}$ and $\lambda_{\max}$.

If the tortuous capillary tube is considered being a straight capillary tube (D_T =1), the Eqs. (42) and (43) reduce to the following equations, respectively.

$$Q=\frac{\pi\Delta P}{128\mu L_0}\frac{D_f\ \lambda_{\max}^4}{4-D_f}\left[1-\frac{16\tau_0\ L_0}{3\Delta P\ \lambda_{\max}}\frac{4-D_f}{3-D_f}-\frac{4-D_f}{3D_f}\left(\frac{4\tau_0 L_0}{\Delta P\ \lambda_{\max}}\right)^4\left(1-\left(\frac{\lambda_{\min}}{\lambda_{\max}}\right)^{-D_f}\right)\right] \tag{44}$$

$$K=\frac{\pi}{128A\mu}\frac{D_f\ \lambda_{\max}^4}{4-D_f}\left[1-\frac{16\tau_0\ L_0}{3\Delta P\ \lambda_{\max}}\frac{4-D_f}{3-D_f}-\frac{4-D_f}{3D_f}\left(\frac{4\tau_0 L_0}{\Delta P\ \lambda_{\max}}\right)^4\left(1-\left(\frac{\lambda_{\min}}{\lambda_{\max}}\right)^{-D_f}\right)\right] \tag{45}$$

Eqs.(44)-(45) indicate that the volumetric flow rate and permeability for a Bingham fluid are very sensitive to the maximum pore size $\lambda_{\max}$ as in the other fluid models such as the Ellis, the power-law and the Newtonian. Eqs. (44) and (45) show that the effects of process variables on the volumetric flow rate and permeability for a Bingham fluid. The larger pore diameter and pore fractal dimension D_f, the larger volumetric flow rate and permeability value. Eqs. (44) –(45) indicate that the volumetric flow rate and permeability for a Bingham fluid will reach possible maximum values as the pore area fractal dimension approaches its possible maximum value of 2 since those quantities, as stated earlier, increase with increasing pore diameter. The pore area fractal dimension D_f = 2 corresponds to a smooth surface or plane or compact cluster [9]. This means that if it is considered a smooth surface or compact cluster or a circle or a square to be the cross-sectional area of a pore, the pore fractal dimension of the cross-section is 2 and the pore volume fraction of the cross-section is 1. Under such a condition the volumetric flow rate and permeability for the Bingham model take their maximum values. Hence, the maximum volumetric flow rate and permeability for a Bingham fluid flowing through the unit cell with a single capillary tube or pore are obtained from Eqs. (44) and (45) as the pore-area fractal dimension, D_f, takes its maximum value of 2.

$$Q = \frac{\pi \Delta P \lambda_{\max}^4}{128 \mu L_0}\left[1 - \frac{32\tau_0 L_0}{3\Delta P \lambda_{\max}} - \frac{1}{3}\left(\frac{4\tau_0 L_0}{\Delta P \lambda_{\max}}\right)^4\left(1 - \left(\frac{\lambda_{\min}}{\lambda_{\max}}\right)^{-2}\right)\right] \tag{46}$$

$$K = \frac{\pi \lambda_{\max}^4}{128 A \mu}\left[1 - \frac{32\tau_0 L_0}{3\Delta P \lambda_{\max}} - \frac{1}{3}\left(\frac{4\tau_0 L_0}{\Delta P \lambda_{\max}}\right)^4\left(1 - \left(\frac{\lambda_{\min}}{\lambda_{\max}}\right)^{-2}\right)\right] \tag{47}$$

Eq. (46) gives totally different result from Eq. (39) with D_T = 1 (and consequently L = L0) although identical equations for other fluid models give approximately similar results.
As mentioned previously, the flow rate equation obtained for a Newtonian fluid flow through the unit cell with a straight capillary tube is the same as that obtained for a Newtonian fluid flow through a tube. For other fluid models namely the power-law and the Ellis models the flow rate equations obtained for flow through the unit cell with a straight capillary tube are approximately similar to those obtained for flow through a tube. Unfortunately the similar agreement between the two flow rate equations for flow of a Bingham fluid through the unit cell with a straight capillary tube (Eq. 46) and through a tube (Eq. 39) is not observed, which is clearly seen in the comparison of Eq. (46) and Eq. (39) with D_T = 1 (and thus $L = L_0$). As can be seen from Eq. (46) the term of $(\lambda_{\min} / \lambda_{\max})^{-2}$ takes a value of 104 as the ratio of $\lambda_{\min} / \lambda_{\max}$ takes a value of 10-2 that is used as a criterion whether a porous medium can be characterized by fractal theory and technique. Therefore, it can be said that the equations of the volumetric flow rate (Eq. 46) and permeability (Eq. 47) for a Bingham fluid flow through the unit cell with a straight capillary tube will not give the correct results since the term of $\lambda_{\min} / \lambda_{\max}$ could not be dropped from those equations completely. In other words, the present approach based on the fractal characteristics of pores in the media is not valid for obtaining the volumetric flow rate of the Bingham fluid and thus permeability.

5. Volumetric Flow Rates with Hydraulic Conductivity in a Single Tortuous Capillary Tube

Eq. (19) expressed in terms of the fractal scaling parameters can be used for obtaining volumetric flow rate of a Newtonian fluid flow in a single tortuous capillary tube. As expressed earlier the tortuosity influences the volumetric flow rates of non-Newtonian and Newtonian fluids as evidenced in Eqs. (18), (19), (33) and (42). On the other hands, the volumetric flow rate of a Newtonian fluid in a converging-diverging duct (see Fig. 1) is given by Balhoff and Thompson [6].

$$q = \frac{g}{\mu}\Delta P \tag{48}$$

where ΔP stands for the pressure drop along the converging-diverging duct, μ the viscosity of the Newtonian fluid and g hydraulic conductivity. The hydraulic conductivity for the converging-diverging duct is given by

$$g = \frac{\pi {R_d}^4}{8 l_0} \tag{49}$$

where Rd is the duct geometric constant and given by

$$R_d = \left(\frac{8 l g}{\pi}\right)\left(0.47{\gamma_R}^3 - 1.34{\gamma_R}^2 + 1.19\gamma_R + 0.68\right) \tag{50}$$

which was numerically determined by Balhoff and Thompson [6] where l is the pore-to-pore distance and γ_R is the aspect ratio and taken to be 0.3. Rd is also equals to the radius of

capillary, R for a straight capillary tube. The converging-diverging duct is schematically shown in Fig. 1. As can be seen from the figure the aspect ratio is 0.3, the pore-to-pore distance is 1 cm, the outside diameter is 0.5 cm and hydraulic conductivity is 6.83×0-5 cm3 [6].

One can obtain the hydraulic conductivity in terms of the fractal scaling parameters by comparing Eq. (19) with Eq. (48) as follows:

$$g = \frac{D_f}{3 + D_T - D_f}\left(\frac{\pi R^{3+D_T}}{2^{4-D_T} L_0^{D_T}}\right) \tag{51}$$

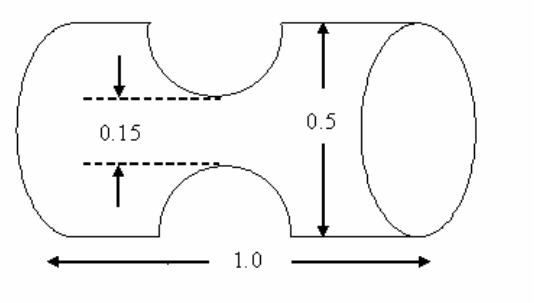

Figure 1. Schematic of axis-symmetric converging-diverging duct

As can be seen from Eq. (51) the hydraulic conductivity is independent of the fluid properties but dependent on the structural parameters (R,L_0 , D_T and D_f of a capillary tube or duct. The volumetric flow rate of a power-law fluid flow through the unit cell with a straight capillary tube, in terms of the fractal scaling parameters, is given by Eq. (18) and can be expressed in terms of the hydraulic conductivity as follows:

$$Q = \left(\left(\frac{n}{3n+1}\right)^n \frac{4\,\pi^{n-1} R^{3(n-1)}\; D_f^{n-1}\left(3 + D_T - D_f\right) g\,\Delta p}{m\left(3 + D_T/n - D_f\right)}\right)^{1/n} = \left(\frac{g}{\mu_F}\Delta p\right)^{1/n} \tag{52}$$

where

$$\mu_F = m\frac{\pi}{4}\left(\frac{3n+1}{n\pi}\right)^n \frac{\left(3 + D_T/n - D_f\right)^n}{D_f^{n-1}\left(3 + D_T - D_f\right)} R^{3-3n}$$

and g is given by Eq. (51).

Eq. (48) is recovered from the above equation by setting $n = 1$ and $m =$ □ with the g given by Eq. (51). The volumetric flow rate of an Ellis fluid flow through the unit cell with a straight capillary tube, in terms of the fractal scaling parameters, is given by (33) and can be expressed in terms of the hydraulic conductivity as follows:

$$Q = \frac{g\,\Delta P}{\eta_0}\left[1 + \frac{4\left(3 + D_T - D_f\right)}{(\alpha+1)\left(3 + \alpha D_T - D_f\right)}\left(\frac{4\left(3 + D_T - D_f\right)}{\pi D_f R^3 \tau_{1/2}} g\Delta P\right)^{\alpha-1}\right] = \frac{g\,\Delta p}{\eta_0}\left[1 + \left(\frac{g}{\mu_E}\Delta P\right)^{\alpha-1}\right] \tag{53}$$

where g is given by Eq. (51) and μ_E is equal to

$$\mu_E = \frac{\pi}{4}\tau_{1/2} D_f R^3 \left(\frac{(\alpha+3)}{4}\right)^{1/(\alpha-1)} \left(\frac{3 + \alpha D_T - D_f}{\left(3 + D_T - D_f\right)^{\alpha}}\right)^{1/(\alpha-1)}$$

The volumetric flow rate of a Bingham fluid flow through the unit cell with a straight capillary tube, in terms of the fractal scaling parameters, is given by (42) and can be expressed in terms of the hydraulic conductivity as follows:

$$Q = \frac{g\,\Delta P}{\mu}\left[1 - \frac{D_f}{3-D_f}\frac{\pi R^3}{3g}\frac{\tau_0}{\Delta P} + \frac{1}{3}\frac{\left(3+D_T-D_f\right)}{\left(3-3D_T-D_f\right)}\left(\frac{\pi D_f R^3 \tau_0}{4g\,\Delta P\left(3+D_T-D_f\right)}\right)^4\left(1-\left(\frac{\lambda_{\min}}{\lambda_{\max}}\right)^{3-3D_T-D_f}\right)\right]$$

The above equation can be rearranged as follows:

$$Q = \frac{g\,\Delta P}{\mu}\left[1 - \frac{1}{3}\frac{\mu_{B1}}{g\Delta P} + \frac{1}{3}\left(\frac{\mu_{B2}}{4g\,\Delta P}\right)^4\left(1-\left(\frac{\lambda_{\min}}{\lambda_{\max}}\right)^{3-3D_T-D_f}\right)\right] \tag{54}$$

where $\mu_{B1} = \pi R^3 \tau_0\left(\frac{D_f}{3-D_f}\right)$ and

$$\mu_{B2} = \pi R^3 \tau_0\left(\frac{D_f}{\left(3+D_T-D_f\right)^3\left(3-3D_T-D_f\right)}\right)^{1/4}$$

As stated previously, the term of $(\lambda_{min}/\lambda_{max})^{-2}$ in Eq. (54) takes a value of 10^4 as the ratio of $\lambda_{min}/\lambda_{max}$ takes the value of 10^{-2}. Therefore, it can be said that the equation of the volumetric flow rate (Eq. 54) for a Bingham fluid flow through the unit cell with a straight capillary tube will not give the correct results since the term of $\lambda_{min}/\lambda_{max}$ could not be dropped from the equation completely.

Here τ_0 is yield stress and g (hydraulic conductivity) is given by Eq. (51). Yield stress fluids require a minimum stress to initiate flow. In order to correctly model flow of these fluids, the equation for flow must accurately predict the applied pressure drop that yields the flow.

After obtaining the volumetric flow rates for the considered fluid models in terms of the fractal scaling parameters, we can also obtain an equation for apparent viscosity of power-law fluids in terms of the fractal scaling parameters easily. In order to obtain the apparent viscosity of the power-law fluid in the unit cell with a straight capillary tube, the strain tensor has to be determined. Therefore, one has to examine the flow of the power-law fluid flow through the unit cell with a straight capillary tube. The only non-vanishing velocity gradient in the tubular flow is dv_z/dr dv_z/dr. The rate of strain tensor reduces to following expression [11].

$$\dot{\gamma} = \sqrt{\frac{1}{2}\left(\dot{\gamma} : \dot{\gamma}\right)} = \sqrt{\left(\frac{dv_z}{dr}\right)^2} = \left|\frac{dv_z}{dr}\right| \tag{55}$$

In tubular flow for all r, $dv_z/dr < 0$; therefore the absolute value of the strain rate has to be equal to $-dv_z/dr$. Thus, from Eqs. (55) and (18) the strain rate in terms of the fractal scaling parameters for the power-law fluid can be written as follows:

$$\dot{\gamma} = \left(-\frac{R}{2m}\frac{dp}{dz}\right)^{1/n} = \frac{3+D_{T/n}-D_f}{D_f}\left(\frac{3n+1}{n\pi}\right)\frac{Q}{R^3} \tag{56}$$

and the apparent viscosity for a power-law fluid is given by

$$\eta_{app} = m\,\dot{\gamma}^{n-1} \tag{57}$$

where m is the consistency index and n the power-law index. Combining Eqs. (56) and (57) yields the apparent viscosity in terms of the fractal scaling parameters.

$$\eta_{app} = m\left(\frac{\Delta P\, R^{D_T}}{2^{2-D_T}\, m\, L_0^{D_T}}\right)^{\frac{n-1}{n}} = m\left(\frac{3+D_{T/n}-D_f}{D_f}\left(\frac{3n+1}{n\pi}\right)\frac{Q}{R^3}\right)^{n-1} \tag{58}$$

Eq. (58) represents the fractal expression for apparent viscosity of power-law fluids. This expression shows the influences of parameters on the viscosity. As can be seen from Eq. (57) the apparent viscosity of power-law fluids depends on the velocity gradient and power-law index and decreases with increasing the velocity gradient since the values of power-law index vary between 0 and less than 1 for pseudo plastic fluids. Furthermore, it is well-known that the velocity gradient depends very much on the pressure gradient and size of geometry. Therefore, every parameter that increases the velocity gradient will cause the viscosity of fluid to decrease. Thus, it can be said that the apparent viscosity of power-law fluids decreases with increasing the pressure gradient and radius of pore as seen from Eq. (58). On the other hand, an increase in the value of the tortuosity fractal dimension, D_T and the length of pore, L_0 will decrease the flow velocity in the pore and thus affects the viscosity of power-law fluid in affirmative way. In other words, a decrease in viscosity of a power-law fluid by increasing shear rate will be hindered by increasing the tortuosity fractal dimension and the length of pore.

6. Results and Discussion

Tortuosity factor can be calculated from the empirical equations that relate tortuosity to porosity in porous media. The tortuosity fractal dimension D_T can be calculated from a relationship between the tortuosity and structural parameters such as R and L_0. There are the number of relationships between tortuosity and porosity as indicated by Chhabra et al. [7]. The tortuosity factor, T, defined as L/L_0. Chhabra et al. [7] reported that the considerable confusion exists in the literature regarding the value and the meaning of tortuosity factor T. Some discussion and equations ($T=\sqrt{2}, T=1/\varepsilon$ and $T=1/\sqrt{\varepsilon}$) regarding tortuosity factor are given in their paper. The following equation was given by Comiti and Renaud [12].

$$T = 1 + B\ln(1/\varepsilon) \tag{59}$$

where ε is the porosity and the value of constant B depends on the shape of packing and of flow particle configuration (for example, B = 0.41 for tightly packed spheres, B = 3.2 for square based parallelpipedal particles of height-to-size ratio equal to 0.1 tightly packed in cylindrical column). Furthermore, Dharamadhikari and Kale [13] claimed that the tortuosity factor is function of the flow rate for polymer solutions.

The relationship between the tortuosity fractal dimension and tortuosity in porous media is given by Yu [14].

$$D_T = 1 + \frac{\ln T}{\ln(L_0/2R)} \tag{60}$$

In two-dimensional space the porosity for Fig. 1 can be obtained as follows:

$$\varepsilon = \frac{V_t - V_p}{V_t} = \frac{0.5\times 0.1 - \pi\times 0.35^2/4}{0.5\times 0.1} = 0.8076$$

where V_t is the total volume of the cylindrical cell and V_p is the volume of spherical particle in the two-dimensional space. The tortuosity can be calculated from Eq. (59) with the use of the obtained porosity and taking B = 0.41, and then the tortuosity fractal dimension can be obtained from Eq. (60). However, in order to obtain the tortousity fractal dimension one needs the radius and straight length of the tortuous capillary. Balhoff and Thompson [6] performed the FEM simulations on the power-law fluid in a converging-diverging duct. They obtained different dimensions for the structural parameters (length and radius of capillary) at each value of power-law index n. For instance, the structural parameters R and L were respectively obtained to be 0.106 cm and 0.731 cm for a value of n = 0.30 while those parameters were found to be 0.097 cm and 0.501 cm for a value of n = 0.80, respectively. Note that in their study the structural parameters vary with power-law index to match the FEM data which shows the weakness of their network model.

In order to compare the present model to the converging-diverging duct approach, the average values of radii and lengths used in that study are taken to be the radius and straight distance of tortuous capillary tube in the present investigation. Therefore, R, L_0 are taken to be 0.102 cm and 0.620 and thus the tortousity fractal

dimension D_T is found to be 1.0752 from Eqs. (59) and (60).

A determined value of the tortuosity fractal dimension from relationships among porosity, tortuosity and the tortuosity fractal dimension can be used in Eq. (52) with n = 1 and D_f = 2, Eq. (52) with D_f = 2 and Eq. (53) with D_f = 2 to obtain the volumetric flow rates versus pressure drops for a Newtonian fluid, a power-law fluid and an Ellis fluid, respectively. The converging-diverging duct can be transformed into a single fractal capillary with the structural parameters, R = 0.102 cm, L_0 = 0.620 cm and D_T = 1.0752 that do not vary with n for the power-law model and for the Ellis model. The determined value for the tortuosity fractal dimension (D_T = 1.0752) is used in the flow rate equations to determine an agreement or a disagreement between the fractal capillary model and the converging-diverging duct approach. Furthermore, values of the tortuosity fractal dimension are varied around the determined value to examine how the volumetric flow rates for the considered fluid models change.

In the converging-diverging duct approach the equation which gives the volumetric flow rate of power-law fluid is given as follows [6].

$$q = \left[\frac{4g}{m\pi R_d^{3-3n}} \left(\frac{n\pi}{3n+1} \right)^n \Delta p \right]^{1/n} \qquad (61)$$

where g is hydraulic conductivity and equal to 6.83×10^{-5} cm^3 and m is consistency index and R_d is duct geometric constant given by Eq. (50). In the converging-diverging duct approach the volumetric flow rate of a power-law fluid as a function of pressure drop is calculated using Eq. (61) with g = 6.83×10^{-5}, m = 1 and Eq. (50).

On the other hand, the fractal expressions are developed based on the fractal nature of tortuous capillaries in a porous media. In other words, it is assumed that the converging-diverging duct can be transformed into a single fractal capillary.

Fig. 2 shows the volumetric flow rate of a Newtonian fluid versus pressure drop for various values of the tortuosity fractal dimension, D_T Fig.2 is depicted using Eq. (52) with n = 1, m = 1 and D_f =2 and Eq. (61) with n = 1 for the fractal capillary model and the converging-diverging duct approach, respectively. As can be seen in Fig. 2 the fractal capillary model and converging-diverging duct approach are in good agreement as the tortuosity fractal dimension has a value around the determined value of 1.0752. The deviation between the two models for flow rate of a Newtonian fluid increases with increasing the tortuosity fractal dimension. Moreover, the deviation slightly increases with increasing pressure drop. In whole computations the hydraulic conductivity is taken to be equal to Eq. (51) in the fractal capillary model equations and 6.83×10^{-5} in the converging-diverging duct approach. In other words, the constant value of g = 6.83×10^{-5} is not used in none of the fractal capillary model equations but the converging-diverging duct approach. In order to compare the converging-diverging duct approach with the fractal capillary model, the volumetric flow rates of power-law fluids obtained from both models (Eq. (61) for the converging-diverging duct approach, and Eqs. (14) and (52) for the fractal capillary model) are drawn in Fig. 3, Figs. 4a and 4b as a function of pressure drop.

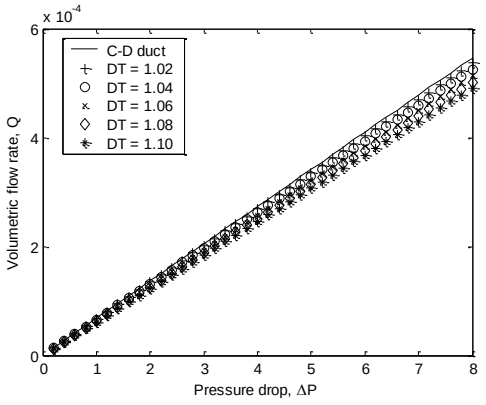

Figure 2. Variation of the volumetric flow rate of Newtonian fluids as a function of pressure drop

The volumetric flow rate for a power-law fluid with n = 0.8 as a function of pressure drop is illustrated in Fig. 3. The figure is depicted using Eq. (52) with D_f =2 and Eq. (71) for the fractal capillary model and the converging-diverging duct approach, respectively. As can be seen in the figure the agreement between the fractal capillary

model and the converging-diverging duct becomes better when values of the tortuosity fractal dimension approaches 1.0. In other words, the deviation between the two models becomes worst as values of the tortuosity fractal dimension go away from 1.0. Furthermore, the deviation between the two models is dependent on the pressure drop and increases with increasing pressure drop. Fig. 4a is sketched using Eq. (14) with the equivalent parameters of $L(\lambda)$ (Eq. 5) for obtaining the volumetric flow rate of a power-law fluid (n = 0.3) flow through a single tortuous capillary tube as a function of pressure drop. Fig. 4b is depicted using Eq. (52) with D_f =2 for the volumetric flow rate of a power-law fluid (n = 0.3) through the unit cell with a straight capillary tube as a function of pressure drop. In both figures volumetric flow rates of power-law fluids versus pressure drop for the converging-diverging duct approach are computed from Eq. (61) with appropriate values of L and R. From the comparison of Figs. 4a and 4b it is clearly seen that the agreement between Eq. (14) and Eq. (61) is much better than that between Eq. (52) and Eq. (61).

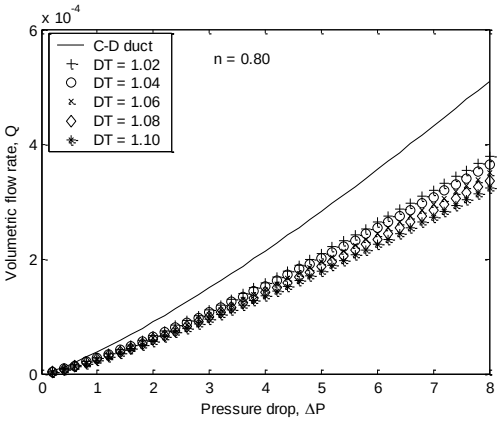

Figure 3. Variation of the volumetric flow rate of a power-law fluid (n = 0.8) as a function of pressure drop

Consequently, the model equations developed for volumetric flow rates of non-Newtonian fluid flows in the unit cell with straight capillary tube can't be correctly used for obtaining volumetric flow rates of those fluid flows through a single tortuous capillary.

The difference between Eq. (14) with equivalent parameters of $L(\lambda)$ and Eq. (52) with substituting Eq. (51) comes from the term of D_f /(3+ D_T /n – D_f). Therefore, the farther a value of power-law index from the unity, the larger disagreement between Eq. (14) and Eq. (52) at each constant value of D_f (D_f is set to be 2 in the present study).

As mentioned previously those equations for Newtonian fluid case can be used for one another for obtaining flow rate as a function of pressure drop.

As can be seen in the figures (Figs. 4a and 4b) the deviation between the two models increases with increasing the tortuosity fractal dimension D_T . From the comparison of Fig. 3 and Figs. 4a and 4b it can be concluded that the deviation, in the volumetric flow rate of power-law fluids obtained from the fractal expression (Eq. 52) and converging-diverging duct (Eq. 61), for the lower power-law index (n = 0.3) is larger than that for the higher power-law index (n = 0.8). Therefore, it can be said that the deviation between the two models increases with decreasing power-law index, which can be evidenced by considering Figs. 2, 3 and 4. Fig. 4b indicates that at low pressure drops the flow rate of power-law fluid with n = 0.3 is very low relative to that of power-law fluid with n = 0.8 at corresponding pressure drop.

Ellis fluids are also examined in terms of the volumetric flow rates as a function of pressure drop to check an agreement or a disagreement between the two models. The volumetric flow rate for an Ellis fluid in the converging-diverging duct approach is calculated from the following equation.

$$q = \frac{g}{\eta_0}\Delta p\left[1+\frac{4}{\alpha+3}\left(\frac{4\,g\,\Delta p}{\tau_{1/2}\pi\,R_d{}^3}\right)^{\alpha-1}\right] \qquad (62)$$

In this equation $g, \tau_{1/2}$, η_0 and α are taken to be 6.83×10^{-5} cm^3, 0.719 Pa, 4.35 Pa.s and 2.47, respectively. These data were experimentally determined by Park (see paper by Balhoff and

Thompson, [6]) for 0.5 % polyacrylamid (separan) solution.

In the fractal capillary model the volumetric flow rate of Ellis fluids is calculated from Eq. (53) with D_f = 2 and Eq. (51). For various values of flow (power) index, α in the Ellis model, the volumetric flow rate of Ellis fluids as a function of pressure drop are computed and shown graphically in Figs. 5, 6 and 7 in attempt to see an agreement or a disagreement between the two models.

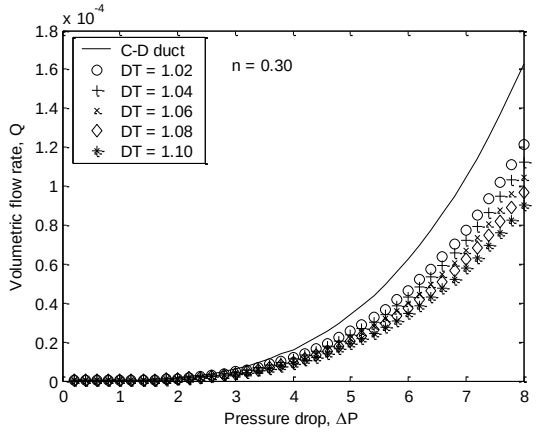

Figure 4a. Variation of the volumetric flow rate of a power-law fluid (n = 0.3) flow through a tortuous capillary tube as a function of pressure drop

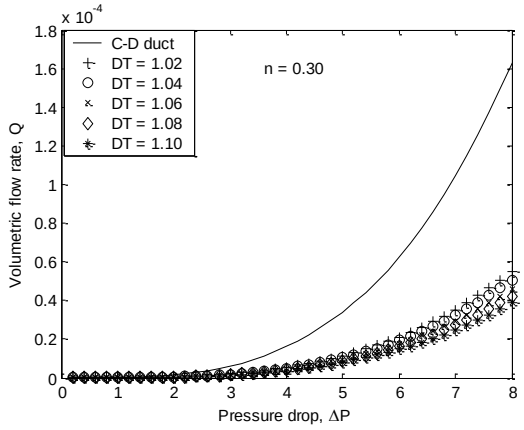

Figure 4b. Variation of the volumetric flow rate of a power-law fluid (n = 0.3) flow through the unit cell with a straight capillary tube as a function of pressure drop

Fig. 5 is depicted for the volumetric flow rate of an Ellis fluid with α = 2.0 versus pressure drop. The figure is drawn using Eqs. (53) and (62) for the fractal capillary model and the converging-diverging duct approach, respectively. As can be seen in the figure the good agreement between the two models is observed for values of D_T around the determined value of 1.0 752. The deviation between the fractal capillary model and the converging-diverging duct approach for an Ellis fluid with α = 2.0 increases with a value of D_T going away from unity. As can be seen in the figure the volumetric flow rate of Ellis fluids calculated from the fractal expression is higher than that calculated from the converging-diverging duct approach for all considered values of D_T. Note that flow rate equation developed for the unit cell with a straight capillary tube (Eq. 53) reduces to the flow rate equation for a single tortuous capillary tube (Eq. 40 with equivalent parameters of $L(\lambda)$ as flow index takes the value of 2.

The volumetric flow rates of Ellis fluids obtained from the converging-diverging duct approach and the fractal capillary model with various values of the tortuosity fractal dimension, as a function of pressure drop, are depicted in Fig. 6 for α = 2.47 and in Fig. 7 for α = 3.0. The identical trend for volumetric flow rates versus pressure drops is observed in the three figures (Figs. 5, 6 and 7). Only difference between these figures is magnitude of the volumetric flow rates of Ellis fluids at the corresponding value of the pressure drop. In other words, the volumetric flow rate of Ellis fluids slightly decreases with increasing flow (power) index, α, in the Ellis model at a constant value of D_T.

As a result, the agreement between the model predictions for volumetric flow rate of a Newtonian fluid flow through a single tortuous capillary tube by the proposed model and those in converging-diverging duct by the FEM is found to be good. Although not comparing to experimental studies, the present fractal capillary model developed for different fluid behaviors is compared with the theoretical studies that have already been compared to the experimental studies.

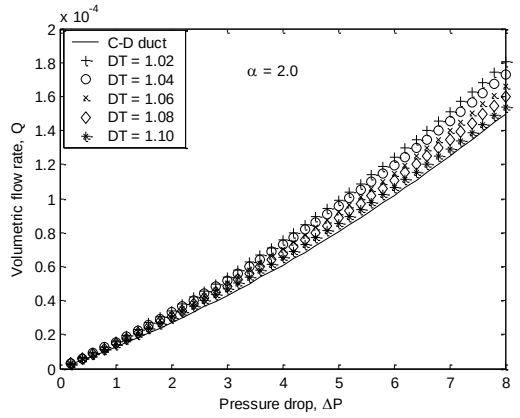

Figure 5. Variation of the volumetric flow rate of an Ellis fluid (= 2.0) as a function of pressure drop

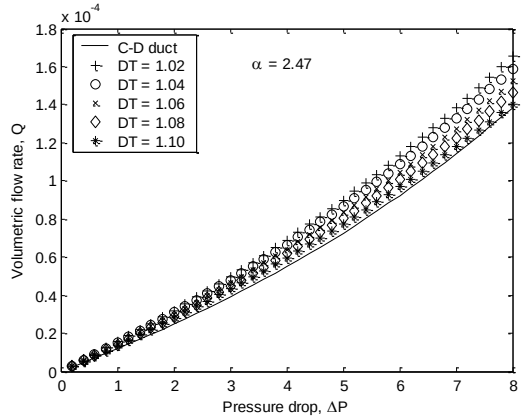

Figure 6. Variation of the volumetric flow rate of an Ellis fluid (= 2.47) as a function of pressure drop

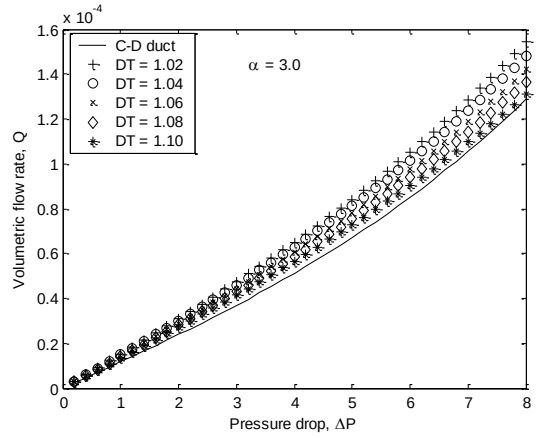

Figure 7. Variation of the volumetric flow rate of an Ellis fluid (= 3.0) as a function of pressure drop

7. Conclusions

To derive flowrate expression for each fluid as a function of pressure gradient is desirable to easily predict amount of fluid passing through porous media. The fractal capillary expressions for calculating volumetric flow rates and permeabilities for Newtonian, power-law and Ellis fluids are developed based on the fractal nature of tortuous capillary. In addition, hydraulic conductivity has also been expressed in terms of fractal scaling parameters. The fractal capillary model is used to model the shear-thinning fluids, including power-law and Ellis fluids. For each fluid the flow rates obtained from both the proposed model and the converging-diverging duct approach supported by FEM are compared to one another to check the accuracy of the developed model. Good agreement between the proposed model and the converging-diverging duct approach is observed at the considered values of the tortuosity fractal dimension for Newtonian fluids. It is also observed that the volumetric flow rate and permeability for Newtonian, power-law and Ellis fluids are very sensitive to the maximum pore size. The flow rates and permeabilities for power-law and Ellis fluids depend on values of the pore-area fractal dimension, the tortuosity fractal dimension and flow indices. The flow rates of power-law fluids increase with increasing power-law index having values between 0 and less than 1.0 but decreases with increasing the tortuosity fractal dimension. On the other hand, the flow rate of Ellis fluid decreases with increasing both flow (power) index in the Ellis model and the tortuosity fractal dimension. It can also be concluded that the volumetric flow rate and permeability increase with increasing both pore diameter and pore-area fractal dimension. The good agreement between the developed model and the converging-diverging duct approach for flow rates of Ellis fluids is obtained at the values of DT around the determined value for all flow indices considered here. It can be concluded that the fractal capillary model can be used to model shear-thinning fluids, including power-law and Ellis fluids with different rheological properties.

8. References

1. Bird, R.B., Stewart, W.E. and Lightfoot, E.N. (2008). Transport phenomena, Revised 2nd Edition, Wiley, New York.

2. Sabiri, N. and Comiti, J. (1995). Pressure drop in non-Newtonian purely viscous fluid flow through porous media. *Chem. Eng. Sci.*, **50:** 1193-1201.

3. Eslami, A. and Taghavi, S.M. (2017). Viscous fingering regimes in elasto-visco-plastic fluids. *J. Non-Newt. Fluid Mech.*, **243:** 79–94.

4. Tijani, H.I., Abdullah, N., Yuzir, A. and Ujang, Z. (2015). Rheological and fractal hydrodynamics of aerobic granules. Bioresource Techn., **186**: 276–285.

5. Shokri, H., Kayhani, M. H. and Norouzi, M. (2017). Nonlinear simulation and linear stability analysis of viscous fingering instability of viscoelastic liquids. *Physics of Fluids*, **29**: 033101 http://dx.doi.org/10.1063/ 1.4977443

6. Balhoff, M.T. and Thompson, K.E. (2006). A macroscopic model for shear-thinning flow in packed beds based on netweork modeling. *Chem. Eng. Sci.*, **61**: 698-719.

7. Chhabra, R.P., Comiti, J. and Machac, I. (2001). Flow of non-Newtonian fluids in fixed and fluidized beds. *Chem. Eng. Sci.*, **56**: 1-27.

8. Yu, B. and Liu, W. (2004). Fractal analysis of permeability for porous media. *AIChE J.*, **50**: 46-57.

9. Yu, B. and Cheng, P. (2002). A fractal permeability model for bi-dispersed porous media. *Int. J. Heat Mass Transfer*, **45**: 2983-2993.

10. Pearson, J.R.A. and Tardy, P.M.J. (2002). Models for flow of non-Newtonian and complex fluids through porous media. *J. Non-Newt. Fluid Mech.*, **102**: 447-473.

11. Bird, R.B., Armstrong, R.C. and Hassager, O. (1987). Dynamics of polymeric liquids, Wiley, New York.

12. Comiti, J. and Renaud, M. (1989). A new model for determining mean structure parameters of fixed beds from pressure drop measurements: Application to beds packed with parallel pipedal particles. *Chem. Eng. Sci.*, **44**: 1539-1545.

13. Dharamadhikari, R.V. and Kale, D.D. (1985). Flows of non-Newtonian fluids through porous media, *Chem. Eng. Sci.*, **40**: 527-529.

14. Yu, B.M. (2005). Fractal character for tortuous stream tubes in porous media. *Chinese Physics Letters*, **22**:158-160.